NOTICE CONCERNING COPYRIGHT RESTRICTIONS

Numerical Simulation of Anhydrite Scaling in Production Well at the Sumikawa Geothermal Field, Japan

Hisao Kato[1], Junko Kamei[1], Koji Kitao[2] and Yoichi Muramatsu[3]

[1]Central Research Institute, Mitsubishi Materials Corporation, 1-297, Kitabukuro-cho, Omiya-shi, Saitama, 330-8508, Japan
[2]Hachimantai geothermal Corporation, 140, Kaminakajima, Hanawa, Kazuno-shi, Akita, 018-5201, Japan
[3]Department of Liberal Arts, Faculty of Science and Technology, Science University of Tokyo, 2641, Yamazaki, Noda-shi, Chiba, 278-8510, Japan

Keywords

Scale, chemical equilibrium, kinetics, numerical simulation

ABSTRACT

The purpose of this study was to characterize the mechanism for formation of anhydrite scale in a geothermal production well. This was accomplished by analyses and numerical simulations of the scaling and production performance. This work was successful because of some important findings that were made. A temperature inversion was observed near the bottom hole of Well SC-1. It was also found that the geothermal fluids feed from two separate zones: one at a higher temperature (300°C) and another at a lower temperature (250°C). It is where these two fluids mix that the anhydrite precipitates. Both the higher and lower temperature fluids that feed SC-1 are saturated with respect to anhydrite. Mixing of the fluids yields supersaturation of anhydrite. Fluid inclusions in anhydrite scale are composed of only liquid inclusion, which indicates that the scale was formed from liquid single phase prior to flashing. This information is consistent with the decrease of saturation index for anhydrite with flashing. The observed concentration of Sr in anhydrite scale is much higher than predicted from experimentally determined equilibrium partioning of Sr between aqueous and anhydrite phases. This indicates that the scale formed under nonequibrium conditions, as found in hot spring chimneys on the East Pacific Rise. In order to calculate scaling with time, we assumed that anhydrite precipitates from well fluid deposits inside of uniform thickness casing. With this assumption, a mathematical model was developed using an isothermal non-steady plug-flow model. The analyses were made using scaling calculations coupled with wellbore simulations. The simulation of history matching, with variable rate constants, led to the rate constant: log$k$=-4.50. Predictions using the optimum rate constants showed that the slight difference in log$k$ (±0.25) sensitively affected the magnitude of decrease in steam rate. Changes in occurrence of scale deposition with decreasing enthalpy, matched the results of simulations using variable rate constants.

Introduction

The Sumikawa Geothermal Field is located within the Hachimantai Volcanic Region, in northeast Japan (Figure 1). The operation of the power plant started in March 1995 with 50 MWe of installed capacity. One of the highest production wells at Sumikwa is Well SC-1 which has shown decreases in flow rate and enthalpy. In order to determine a cause for this declined productiivity, we made studies and found anhydrite scaling in the wellbore to be one of the causes. In general, scaling in wellbores occurs due to the change in the degree of saturation with respect to scale-forming minerals through the physical processes of boiling or mixing with the different fluid pHs, other chemical features, temperature, and so on (eg. Akaku, 1988; Benoit, 1989; Todaka *et al.*, 1995; Ajima *et al.*, 1998). Estimations/predictions of blocking time play an important role in the management of steam production and planning for workovers. Calcium carbonate is a well-known scale-forming mineral in wellbores. The prediction of the amount of deposition of calcium carbonate using chemical equilibrium calculation is reported by Armannsson (1989), Reed (1989), and Herras *et al.* (2000). Although the precipitation of mineral during upflow of geothermal fluid in wellbores might be out of chemical

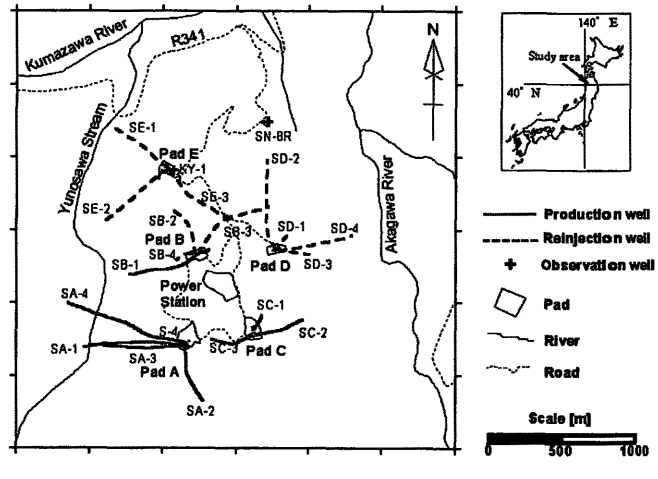

Figure 1. Location map at the Sumikawa geothermal field.

equilibrium owing to rapid flow, little is known about the kinetics of the fluid flow. Therefore, a numerical simulation using kinetics is required to accurately predict the extent of deposition. The purpose of this study is to examine the production performance associated with scale formation. This paper shows the mechanism of scale formation based on the production history and well logging of Well SC-1 and analysis of scale. Moreover the numerical simulations of scaling and discharge rates were made using the scale simulator by the non-steady plug-flow model developed in this study and a current wellbore simulator.

Production History

Well SC-1 is a vertical well with 2,486 m depth. Static temperature profiles measured prior to steam exploitaition and its casing program are shown in Figure 2. Temperature inversion was clearly observed below 2,300 m depth and temperature difference between the higher temperature zone and the lower one was about 50°C. Feeds from both temperature zones were recognized from PTS logging during discharge. Changes in flow rates and wellhead pressure with time are shown in Figure 3. Flow rates and wellhead pressure decreased with time from November 1994 to September 1998 down to about 70% of maximum values. In September 1998, a work-over was made to ream out scale in the wellbore. Shortly after the work-over, the productivity was recovered to some extent. Decrease in flow rates still continued. The decline rate decreased with time and the flow rates have been stable since the latter part of 1999.

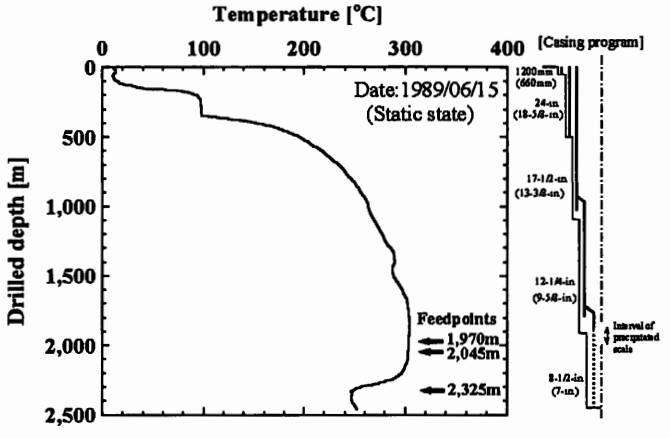

Figure 2. Temperature profile at the static state and casing program for well SC-1.

Changes in temperature from enthalpy calculations and a quartz geothermometer (Fournier and Potter, 1982) are compared in Figure 4. Enthalpy temperatures were somewhat higher than the quartz geothermometer readings from Nov.1994 to 1998, which means that the discharge condition was under excess enthalpy. Both enthalpy and quartz geothermometer temperatures decreased with time and they were almost the same after the latter part of 1998. Truesdell and Lippmann (1998) describe inlet vapor fraction (IVF) as it is fed into a two phase reservoir as follows:

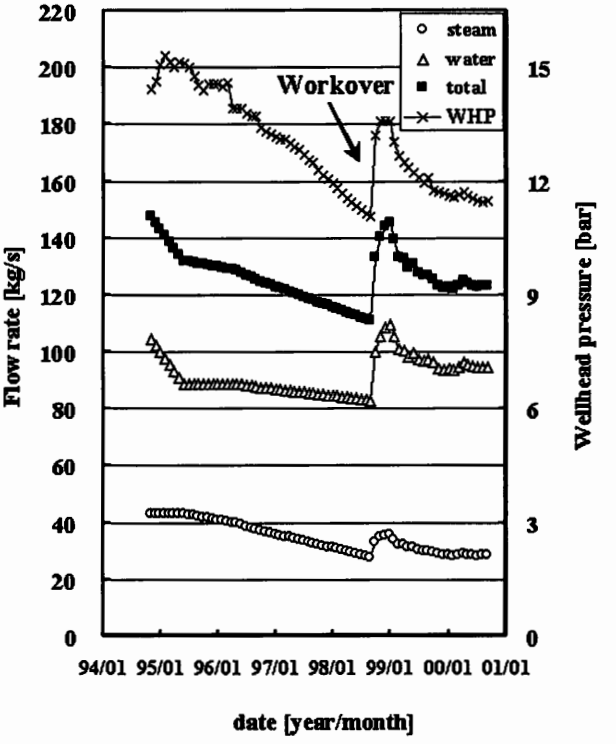

Figure 3. Changes in flow rates and wellhead pressure (WHP) with time for well SC-1.

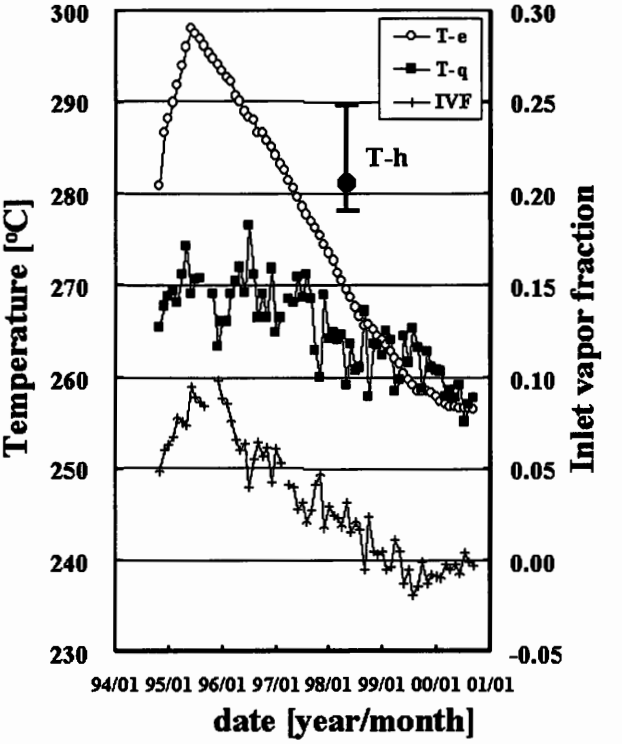

Figure 4. Changes in temperature from enthalpy (T-e) and quartz geothermometer (T-q; Fournier and Potter, 1982), and inlet vapor fraction (IVF, see text) with time, well SC-1. Also shown homogenization temperatures of fluid inclusions (T-h) in anhydrite scale. T-h shows the average and the range measured.

$$IVF = \frac{H_{total} - H_{inlet}}{\lambda_{inlet}} \quad (1)$$

where H_{total}, H_{inlet}, λ_{inlet} are the measured flowing enthalpy, liquid enthalpy fed (calculated from geochemical thermometer), and the latent heat respectively. IVF is also shown in Figure 4. IVF was the maximum value, 0.10 at the maximum enthalpy. IVF showed higher values at the time of excess enthalpy. It is inferred that two phase feed occurs at the higher temperature zone; while single liquid feed occurs at the lower zone.

Analysis of Scale

Scaling occurred at about the 120 m level shortly after mixing between the higher and lower temperature fluids (from the work-over in September 1998). Samples of scale fragments were collected with the junk subset above the tri-cone bit at work-over. The results of thin layer, x-ray diffraction, and chemical analyses are shown in Figure 5 and Table 1 respectively. Scale is pinkish or pale brown colors, and occurs as layered structure (Type A) and massive one (Type B). The above analyses showed

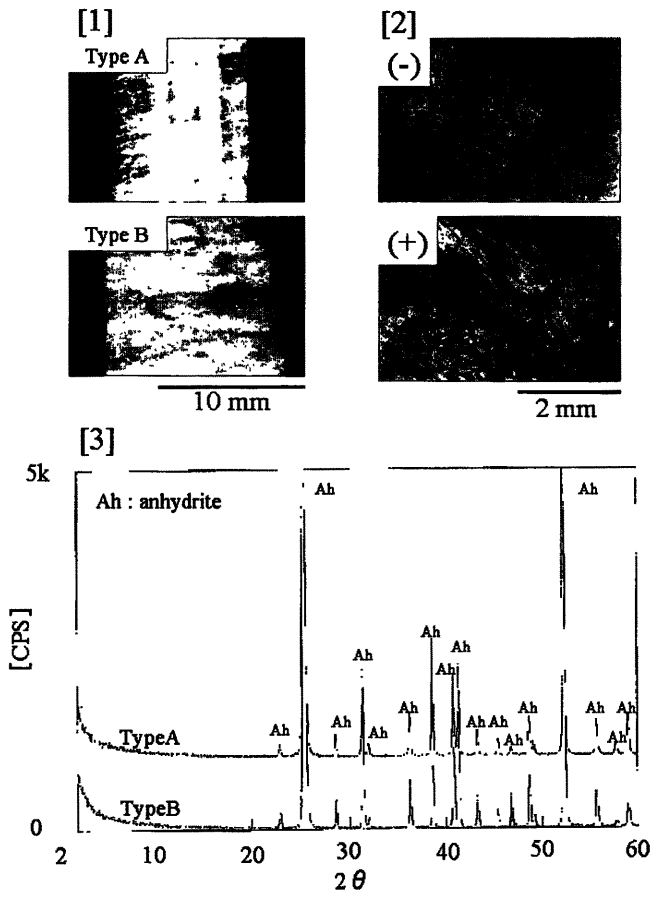

Figure 5. [1] Photograph of the scale of type A and Type B. Type A is a layered structure, and Type B is not a layered one. [2] Photomicrograph of the scale of Type A. (-) and (+) show the images of single nicol and crossed nicols respectively. [3] X-ray diffraction chart of the scale.

Table 1. Chemical composition of the scale.

	wt.%
SiO_2	0.21
Al_2O_3	0.09
Na_2O	0.02
K_2O	<0.01
CaO	41.31
SrO	0.30
MgO	0.05
SO_3	56.03
Ig-loss	1.45
$(CO_2)^*$	(0.13)
Total	99.46

* CO_2 is included in Ig-loss.

that the scale was composed of a single phase of anhydrite. The measurements of density and porosity were 2,899 kg/m^3 and 2.76% respectively. Density of the pure anhydrite is 2,970 kg/m^3 and the measured value is consistent with the theoretical one. Natural anhydrite (eg. Kuroko ore deposits, ocean floor hydrothermal ore deposits) contain Sr instead of Ca (Shikazono *et al.*, 1983; Shikazono and Holland, 1983). Shikazono and Holland (1983) experimentally present the Sr partition coefficient between anhydrite and solution. The partition coefficient (K_d) is defined as follows:

$$K_d = \frac{X_{SrSO_4} / X_{CaSO_4}}{m_{Sr^{2+}} / m_{Ca^{2+}}} \quad (2)$$

where X_i and m_i are mole fraction for mineral, and molality in solution respectively. The Sr partition coefficient based on anhydrite scale and hot water (Table 2) of Well SC-1, is shown in Figure 6 (overleaf) with the results of experimental data and the chimney at the midocean ridge (Shikazono and Holland, 1983). The Sr partition coefficients of the experimental data carried out under equilibrium state are below 0.4, while those of the scale of Well SC-1 and the chimney of the midocean ridge are around 1.0. The environment of formation of the scale is similar to that of the chimney in a view of precipitation during a rapid flow. The discrepancy between experimental products and minerals formed naturally, indicates that the anhydrite scale was formed under non-equilibrium state. Photomicrographs of fluid inclusions of anhydrite scale and results of their homogenization temperature measurements are shown in Figure 7 and Figure 4 respectively. Fluid inclusions were observed as elliptic or irregular shapes under 20μm in diameter. The inclusions observed were composed of liquid-rich-phase inclusion not accompanied with vapor-rich inclusions, which indicates that the anhydrite-forming fluids were liquid single phase but not two phase. The homogenization temperatures range from 279 to 290°C, which correspond to the temperatures for enthalpy rather than those from the quartz geothermometer.

Table 2. Chemical composition of hot water in well SC-1 under the atmospheric pressure.

Date		1997/12/3
pH	[-]	7.5
EC	[μScm^{-1}]	2,350
Na	[mgkg^{-1}]	372
K	[mgkg^{-1}]	63.2
Ca	[mgkg^{-1}]	39
Mg	[mgkg^{-1}]	<0.1
Sr	[mgkg^{-1}]	0.03
Al	[mgkg^{-1}]	2.0
Fe	[mgkg^{-1}]	0.05
Cl	[mgkg^{-1}]	549
SO_4	[mgkg^{-1}]	131
HCO_3	[mgkg^{-1}]	46
B	[mgkg^{-1}]	249
SiO_2	[mgkg^{-1}]	823

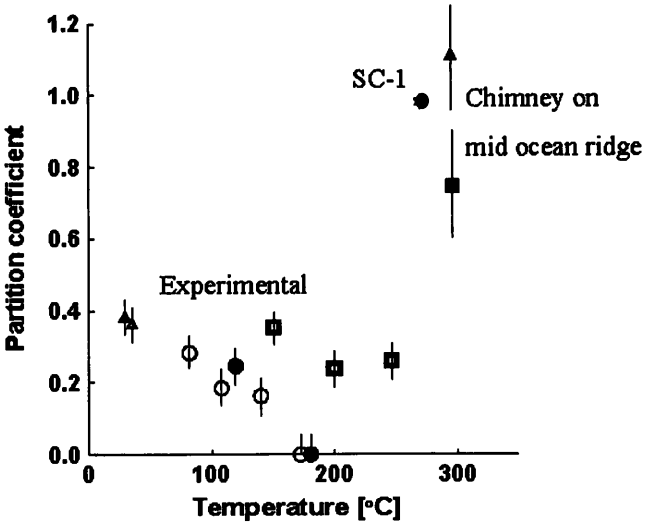

Figure 6. Sr partition coefficient between anhydrite and water of well SC-1. The data of experimental and chimney on the mid ocean ridge are derived from Shikazono and Holland (1983). Sr partition coefficient of the well SC-1's anhydrite is much higher than the experimental data under chemical equilibrium.

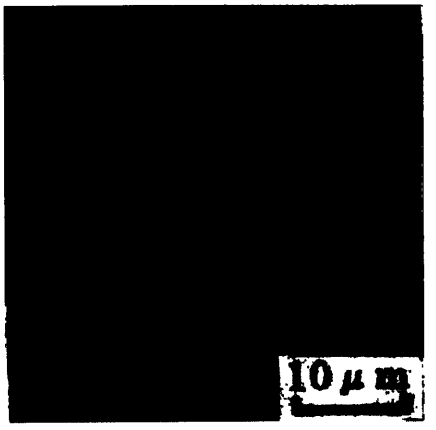

Figure 7. Photomicrograph of liquid-rich inclusion in anhydrite scale from well SC-1.

Well Logging

PTS loggings during discharge were made in November 1988 and in October 2000. The more recent measurements are shown in Figure 8. Four feedpoints were located between 2,000 m and 2,400 m depth. The main feedpoints were identified at the 2,045 m and 2,325 m depths. Fluid temperature changes around the 2,045 m depth in the temperature profile. The inflow ratio between the high and low temperature fluids is about 1:4. The mixed fluid temperature from mixing to flash point is stable at 259°C, which corresponds to the temperatures of enthalpy and the quartz geothermometer. The flash point is around the 1,310 m depth. Irregularity in the rpm of the spinner between the 1,700 m and 1,900m depths is due to the change in fluid velocity from the presence of slotted liner and the change in welllbore diameter.

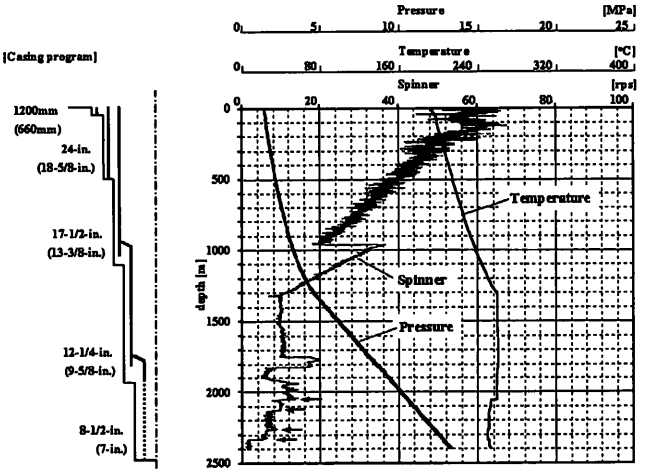

Figure 8. Pressure, temperature and spinner profile during discharge, for well SC-1 (October 3, 2000). The arrow shows the individual feedpoint.

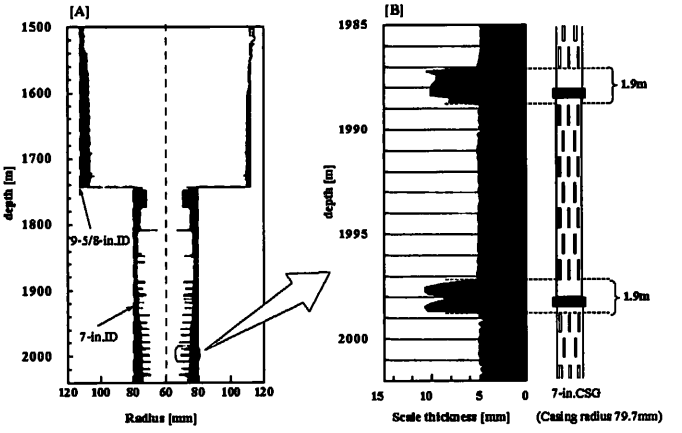

Figure 9. Caliper logging of well SC-1 (September 16, 2000.) [A] shows the whole interval of scale deposition. [B] shows the enlargement at 7-in. slotted liner casing. Scale is far thicker at the connection of casing pipe without slots.

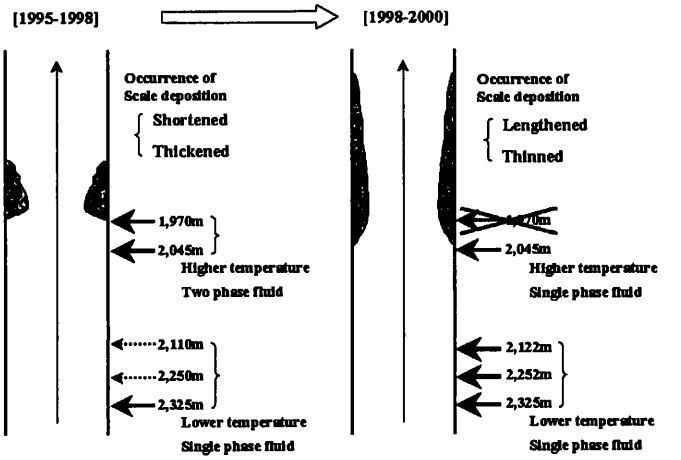

Figure 10. Temporal changes in the occurrence of anhydrite deposition and feedpoints, well SC-1. Solid arrow shows the main feedpoint, while break one does pretty small.

Two years after the work-over, caliper logging was carried out in September 2000 (Figure 9). The purpose of this logging was to find the extent of scale deposition and to plan the timing for future work-overs. The scale appears between 1,740m and 2,040m depth in the 7-in. casing, and between 1,530m and 1,740m depth in the 9 5/8-in. casing. Their maximum thickness is 10mm in the 7-in. casing, and 5 mm in the 9 5/8-in. casing. At the upper of the 7-in. casing between 1,740m and 1,850m depth, the scale thickness is thicker upwards. Moreover a pulse-like reduction of diameter was observed at 10 m intervals in the 7-in. casing. That interval corresponds to the length of a casing pipe. At the connection of pipes where the slotted liner is not present, scale deposition rate is more rapid.

Temporal changes in the occurrence of anhydrite deposition and feedpoints for Well SC-1, based on production history and wellbore surveys, are shown in Figure 10. Flowing enthalpy was higher between 1995 and 1998. The higher temperature fluids from 1,970m and 2,04m depths and the lower ones from 2,110m, 2,250m, and 2,325m were fed into the wellbore. The inflow rates from 2,110m and 2,25 m were relatively low. At the time, the scaling in the 9 5/8-in. casing was not present, and scaling occurred at the short and limited section in the 7-in. casing and its deposition rate was relatively rapid. On the other hand, flowing enthalpy was lower between 1998 and 2000. Inflow of the higher temperature fluids was restricted only from the 2,045 m depth, and the inflow ratio between the higher temperature fluids and the lower ones temporally changed from 3:7 to 2:8. It is proposed that the cause of disappearance of the higher temperature feed at 1,970 m depth was plugging, due to scaling. At the time, scaling was spread upwards to inside of the 9 5/8-in. casing, and the scale thickness became relatively thin.

Modeling Based on Chemical Equilibrium

Saturation Index of Anhydrite for Sumikawa Reservoir Fluids

The precipitation-dissolution reaction with respect to anhydrite is defined as follows:

$$CaSO_4 = Ca^{2+} + SO_4^{2-} \quad (3)$$

Solubility of anhydrite decreases with temperature increase and is different from that of many silicate minerals. Chemical equilibrium calculations using SOLVEQ-CHILLER (Reed, 1982) were made for the Sumikawa production fluids to obtain the saturation index (logQ/K) of anhydrite for the Sumikawa reservoir fluids. The relationship between activity products (logQ) of $Ca^{2+}$and SO_4^{2-} for the representative well fluids (wells SC-1, S-4, and SB-1), and anhydrite solubility are shown in Figure 11. Activity products for Ca^{2+} and SO_4^{2-} were calculated and their values lie closely above the anhydrite solubility curve, which means that reservoir fluids are almost saturated with respect to anhydrite. Strictly, the fluids of Well SC-1 are, however, supersaturated by +0.05-0.30 in logQ.

As mentioned above, the higher temperature fluids from the shallower level and the lower fluids from the deeper level were

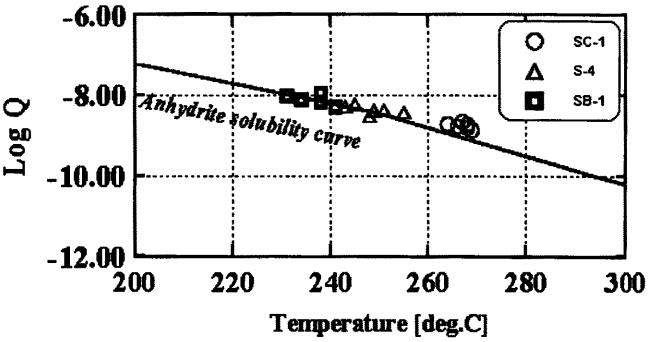

Figure 11. Activity products (logQ) of Ca^{2+} ad SO_4^{2-} for the Sumikawa geothermal fluids (wells SC-1, S-4, and SB-1), and anhydrite solubility curve. The Sumikawa geothermal fluids are almost saturated with respect to anhydrite.

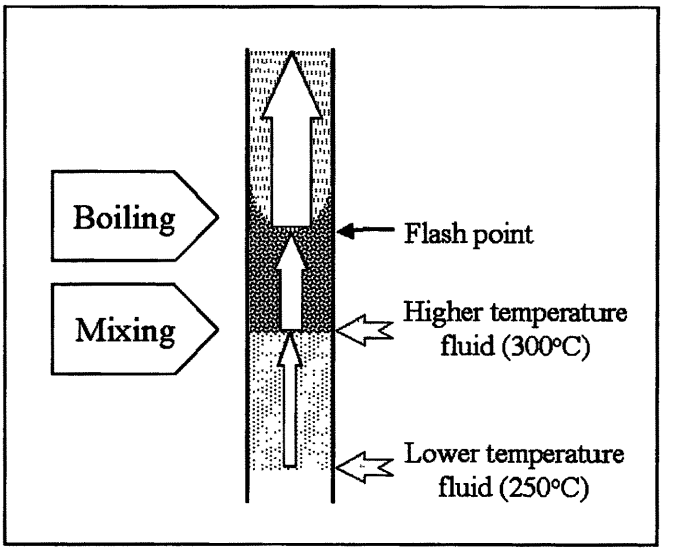

Figure 12. Schematic illustration showing physical processes (mixing and boiling) in the wellbore during discharging. Lower temperature fluid from greater depth and higher temperature fluid from shallower depth enter the well. After mixing, boiling occurs at a shallower depth.

fed respectively into the SC-1 wellbore. Two different physical processes of mixing and boiling occur during upflow in the wellbore (Figure 12). Using two models (mixing and boiling), changes in saturation index of anhydrite with the individual physical process were analyzed as follows:

Mixing Model

Changes in the log of Q/K for anhydrite as a function of the mixing ratios between the higher and lower temperature fluids was analyzed in the mixing model. The assumptions of the model are as follows:

i) The individual end components to mix are the higher temperature (300°C) fluid and the lower temperature (250°C) fluid respectively.

ii) The individual end member fluid is saturated with respect to anhydrite.

Measured data on chemical compositions of both the higher temperture fluids and the lower ones for well SC-1 were not present. Hence the following two cases were substituted for the chemical compositions of the individual end member fluids.

Case 1: The data of the other Sumikawa wells which are around 250°C and 300°C in the reservoir were used.

Case 2: The data of Well SC-1 were modified to be almost saturated with respect to anhydrite at 250°C and 300°C respectively.

The calculation results in the mixing model are shown in Figure 13. Although the individual end component fluids are almost saturated (logQ/K=0) following the above assumption, the mixing fluids are supersaturated (logQ/K>0). The maximum saturation index of anhydrite is 0.40 (Case 1) and 0.20 (Case 2), where the mixing ratio is 0.7 (Case 1) and 0.6 (Case 2). The calculation results of the mixing fluids on saturation index of anhydrite agree with the measured data (log Q/K=0.05 to 0.30) from Well SC-1.

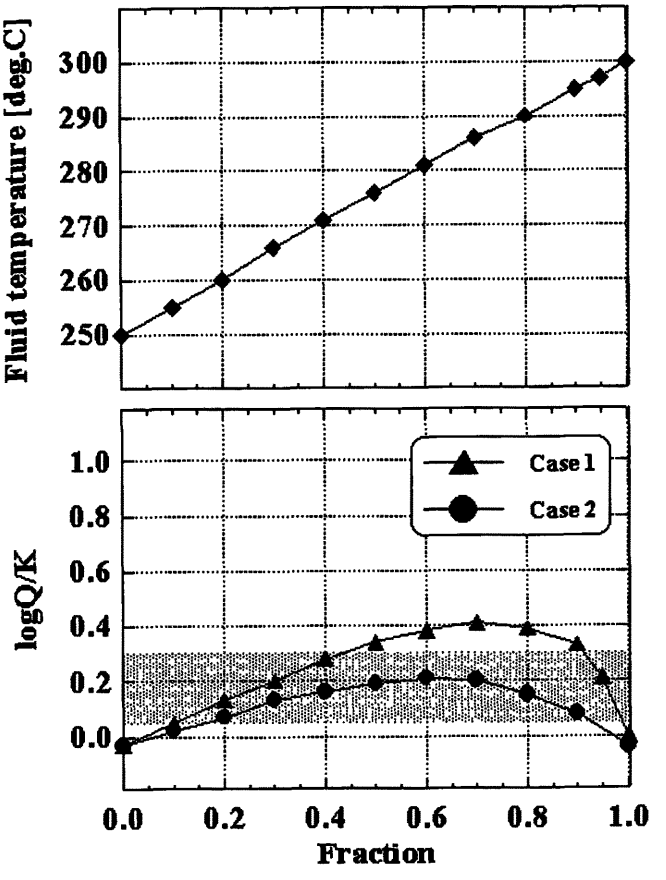

Figure 13. Computed fluid temperature and logQ/K of anhydrite after mixing between lower (250°C) and higher temperature (300°C) fluids. Fraction represents the proportion of higher temperature fluid to the mixed fluid. The other Sumikawa fluids data (Case 1), and the modified fluid from well SC-1 (Case 2) are used as each end member fluid. In both cases it is assumed that the end member fluids are almost saturated with respect to anhydrite. The shadow zone represents the range of logQ/K calculated from the measured values of well SC-1.

The relationship between the solubility product of anhydrite, and the activity product of the solution mixed with the two fluids saturated with anhydrite at 250°C and 300°C, respectively, are shown in Figure 14. With the y-axis expressed linearly, the solubility curve of the anhydrite is concave upwards. Therefore the mixing between the fluids above the solubility curve (saturated with respect to anhydrite) leads the mixed fluid to be supersaturated. The mixing between the waters with the different temperature plays an important role in anhydrite deposition in the wellbore of SC-1. Akaku (1988) also reported the similar formation mechanism of anhydrite scale in a wellbore at the Fushime Geothermal Field, Japan.

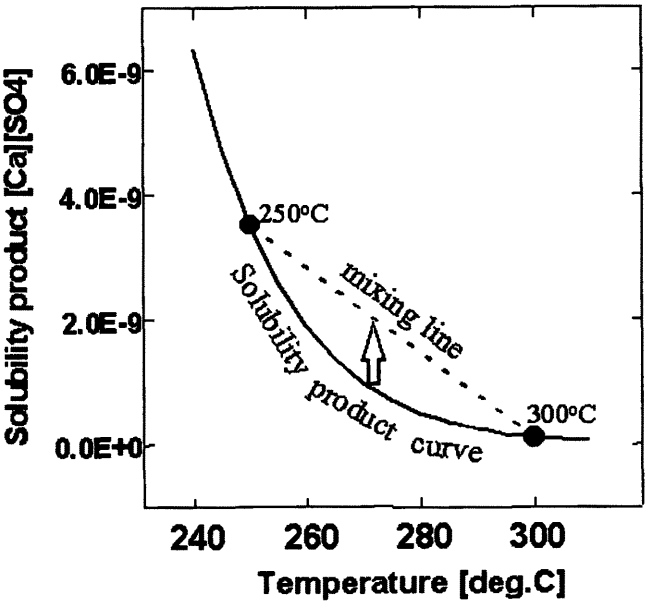

Figure 14. Relationship between the solubility product of anhydrite and the activity product of the solution mixed with two fluids saturated with anhydrite at 250°C and 300°C respectively. Mixing fluids (on the mixing line) are supersaturated with respect to anhydrite because the solubility product curve is concave upward.

Boiling Model

Chemical equilibrium calculations were made from the boiling model, using the data on fluid chemistry and production logging in 1988. Temperature profile and log Q/K calculations are shown in Figure 15. In the boiling model, boiling starts at the 1,355 m depth and 268°C, based on the measured data and log Q/K of anhydrite in liquid water after steam separatation was calculated using a temperature decrease of 10° per step. Chemical compositions of liquid water prior to boiling were used to calculate total discharge from chemical and gas compositions of separated water and steam by SOLVEQ. After boiling, separated steam was allowed to coexisted with separated water, within the system. Minerals supersaturated during the calculation were not precipitated and not separated from liquid water. The calculation results show that log Q/K of anhydrite was +0.25

prior to boiling, and after boiling log Q/K clearly decreased upwards. The reason for this is that the solubility increase with temperature decrease is more effective than the concentration increase with boiling. Consequently it is concluded that anhydrite scale was formed prior to boiling. That agrees with the results of observation of fluid inclusions.

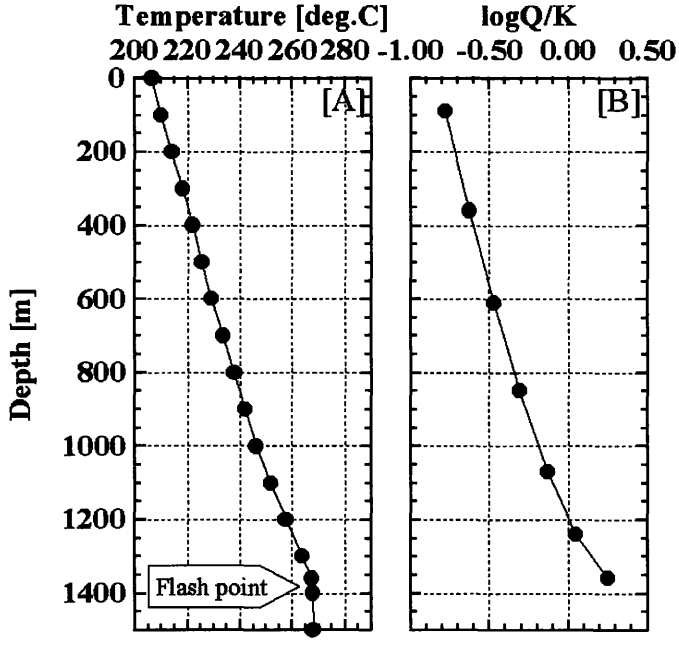

Figure 15. Measured temperature profile during production [A] and computed logQ/K at the boiling model [B] logQ/K of anhydrite decreases with decreasing depth because of increasing solubility with decreasing temperature.

Modeling Based on Kinetics

Modeling of Anhydrite Scaling

A schematic illustration of the model for scale formation inside of the production wellbore is shown in Figure 16. In this model the assumptions are as follows:

i) Scale thickness is equal in a unit section and the surface of crystal growth is parallel to that of the casing pipe.

ii) Fluid temperature is constant during precipitation.

iii) The precipitation rate is proportional to the rate constant, surface area to precipitate, and extent of saturation with respect to a certain mineral (Rimstidt and Barnes, 1980).

iv) First order kinetics is used in the rate equation.

The mass balance equation for the concentration of Ca^{2+} and SO_4^{2-} in liquid water with anhydrite precipitation over a minute distance (Δx) and a minute time (Δt) based on an isothermal, non-steady, plug-flow model is as follows:

$$(C_{x+\Delta x} - C_x)A_0 u \Delta t \rho_f + (C_{t+\Delta t} - C_t)A_0 \Delta x \rho_f = kA_1\left(\frac{C_{eq} - C_t}{C_{eq}}\right) \quad (4)$$

where A_0, A_1, C, C_{eq}, k, u, and ρ_f are cross sectional area fluid passes through, surface area to precipitate, concentration, equilibrium concentration, rate constant, fluid velocity, and fluid density respectively.

Cross sectional area (A_0) and surface area (A_1) are expressed using the radius (r) of the wellbore as follows:

$$A_0 = \pi r^2 \quad (5)$$

$$A_1 = 2\pi r \Delta x \quad (6)$$

Substituting Eq.(5) and (6) for Eq.(4), Eq.(4) becomes as partial differential equation

$$\frac{\partial C}{\partial t} + u\frac{\partial C}{\partial x} = k\frac{2}{r\rho_f}\left(1 - \frac{C}{C_{eq}}\right) \quad (7)$$

Eq.(7) depicts a governed equation on temporal and spatial changes in concentration in water with precipitation in the process of fluid flow.

The relationship between the amount of precipitation and reduction of wellbore diameter is expressed as follows:

$$(1-\phi)\Delta x \rho_s \pi\left(r_t^2 - r_{t+\Delta t}{}^2\right) = -k2\pi r_t \Delta x\left(1 - \frac{C_t}{C_{eq}}\right)\Delta t G \quad (8)$$

where ϕ, ρ_s, and G are scale porosity, scale density, and gram formula weight of anhydrite respectively. Left and right hand

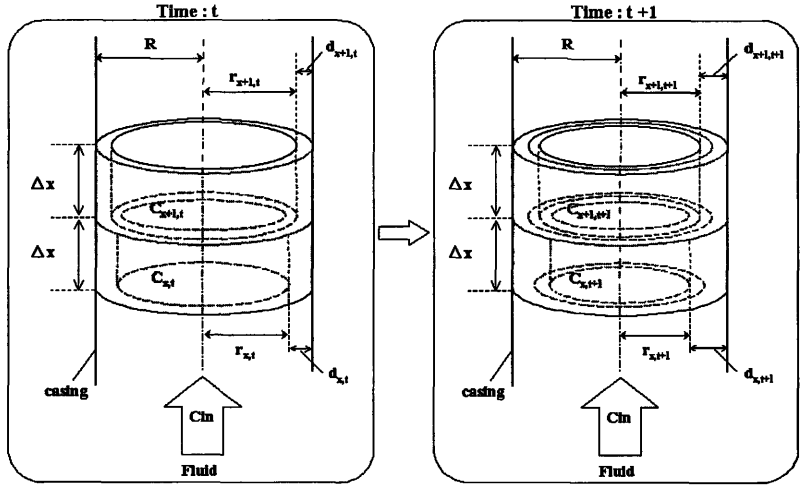

Figure 16. Schematic illustration of the model on scale formation in production wellbore.

sides of Eq.(8) means weight of scale calculated from reduction of wellbore diameter, and rate equation respectively. Conveniently

$$\xi_t = r_t^2 \tag{9}$$

Substituting Eq.(9) for Eq.(8), Eq.(8) becomes as partial differential equation

$$\frac{\partial \xi}{\partial t} = k\frac{2\sqrt{\xi}}{\rho_s}\left(1-\frac{C}{C_{eq}}\right)\frac{G}{1-\phi} \tag{10}$$

Eq.(10) represents a governed equation on temporal change in wellbore diameter with precipitation.

From Eq.(7) and (10), scale thickness at a certain time and distance is defined by

$$d_{t,x} = R - \sqrt{\xi_{t,x}} = R - r_{t,x} \tag{11}$$

where R is half of the wellbore diameter prior to precipitation, or the inner radius of the casing pipe.

The chemical formula of anhydrite is expressed as a two component system of Ca and SO_4. Treatment of C and C_{eq} in Eq.(4), (7), (8), and (10) are referenced from Granbakken *et al.* (1991), as follows:

$$C = \left(m_{Ca^{2+}} \cdot m_{SO_4^{2-}}\right)^{\frac{1}{2}} \tag{12}$$

$$C_{eq} = \left(\frac{K}{\gamma_{Ca^{2+}}\gamma_{SO_4^{2-}}}\right)^{\frac{1}{2}} \tag{13}$$

where m, γ, and K are molality, activity coefficient, and equilibrium constant respectively.

Procedure for Calculation

Scale formation with spatial and temporal changes, and production performance were analyzed in this study. The simulator (we call scale simulator which is based on the equations mentioned above) was used to calculate scale formation. On the other hand, WELBOR (Pritchett, 1985) as a current wellbore simulator was used for production performance. A list of input parameters is shown in Table 3. All the parameters including the rate constant were based on the measured data. Input and output parameters required in the simulations are as follows:

Wellbore Simulation

Input parameters	constants	productivity index, bottom hole pressure, formation temperature
	variables	enthalpy, wellbore diameter
	unknown	production rate
Output parameters		wellhead pressure, flow rate of steam and water, fluid velocity, flash point

Scale Simulation

Input parameters	constants	density of fluid and scale, porosity of scale
	variables	section of scale formation, equilibrium concentration, concentration prior to precipitation, fluid velocity
	unknown	rate constant
Output parameters		scale thickness, concentration after precipitation

After flashing, anhydrite precipitation is restricted as mentioned above. Hence, scale simulation was made up to the flash point. The period of simulation was from October 1998 (workover) to Septemper 2000 (Caliper logging). Production performance associated with scale formation was analyzed as an unknown parameter, rate constant (log k), and the calculatied values were compared with the measured data (history matching). Prediction of the production rate associated with scaling for four years was made using the optimum log k obtained from the history matching.

Calculation Results and Discussion

History Matching

Results of simulations are shown in Figure 17. Scale thicknesses became thinner upwards regardless of the value of log k. Scale thickness at greater depth increased as log k increased, while

Table 3. Parameters used in the simulation.

			The history matching	The prediction
WELBOR	Production index	(kg/s)/bar	30	30
	Bottom hole pressure	bar	125	125
	Formation temperature	°C	0-550m:10, -900m 240, -2,100m:255, 2,100m-:300	0-550m:10, -900m:240, -2,100m.255, 2,100m-:300
	Enthalpy	kJ/kg	initial condition : 1163.3 1,163.3 – 1116.9	1,116.9
	Well geometry	m	initial condition : casing profile	initial condition : based on caliper logging data (Sep-16,2000)
	Interval of scale deposition	m	initial condition : 0	initial condition : 1,522-2,050m
	Flow rate	kg/s	initial condition : 140.9	initial condition : 120.4
Scale simulator	Rate constant	mol/sm^2	logk= -4.00, -4.25 , -4 50, -4.75 , -5.00 , -6.00	logk= -4.25 , -4.50, -4.75
	Fluid density	kg/m^3	767.8	767.8
	Scale density	kg/m^3	2,889	2,889
	Scale porosity	-	0.0280	0.0280
	Equilibrium concentration of fluid	mol/kg	initial condition : 9.13×10^{-5} $9.13\times10^{-5}\sim1.19\times10^{-4}$	1.19×10^{-4}
	Concentration of inlet fluid	mol/kg	initial condition : 1.03×10^{-4} $1.03\times10^{-4}\sim 1.39\times10^{-4}$	1.39×10^{-4}

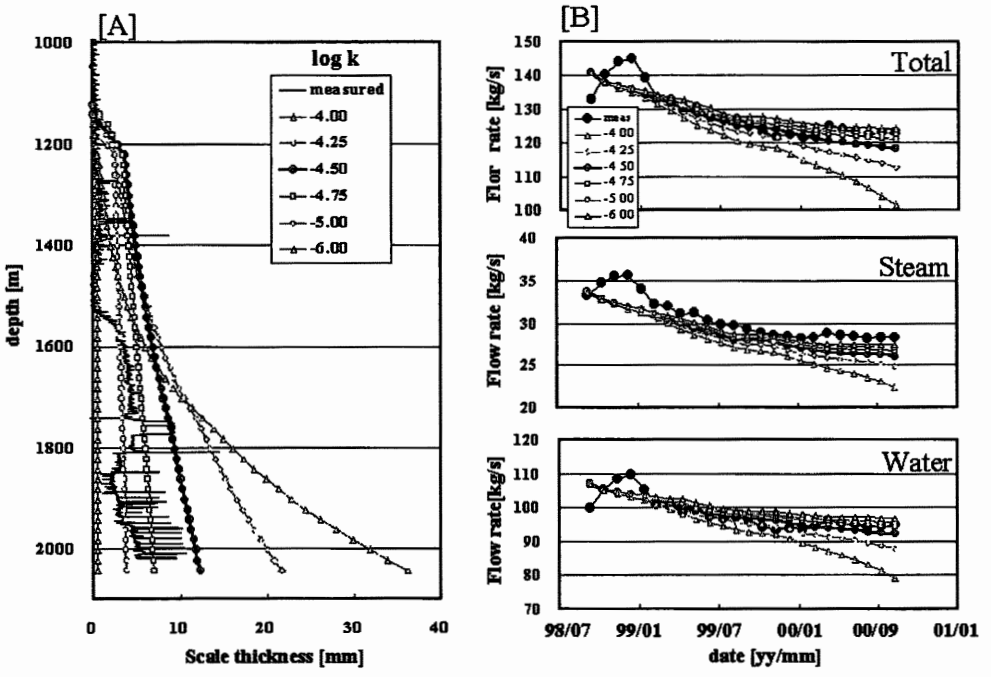

Figure 17. Results of simulations on history matching between the measured data and the computed values with variable rate constants, logk. [A] shows the thickness of scale with depth after two years. [B] shows the changes in flow rates (total, steam and water) with time.

Prediction

Results of the simulation (prediction) are shown in Figure 18. Judging from the history matching, it is appropriate that the optimum rate constant (log k) is -4.50. The prediction analyses were made for log = -4.25, -4.50, and -4.75. In Figure 18 flow rates and wellhead pressures are normalized by individual initial values and scale thickness shows the maximum values. When wellhead pressure falls below 5 bar the production rates decrease, and the calculation was over (eg. after 39 months at log k=-4.25).

In the case of log k=-4.50, the maximum scale thickness increases linearly with time, and becomes 40 mm after four years. The decline in flow rates and wellhead pressure associated with scaling increase with time. The steam rate becomes 90% of the initial value in two years, and 60% in four years.

The rate constant is an important and indispensable parameter in kinetics. In the predictions, a difference of 0.5 units in log k gave a significant difference in the calculation results of flow rates and scale thickness. For example, in the case of log k=-4.25, the steam rate becomes 50% in three years, while at log k=-4.75, the rate is 90%. In application of the rate constant, matching with measured data or references to experimental data are required.

that at shallower depths drastically decreased. In general, the rate constant increases as temperature increases for a given mineral (Rimstidt and Barnes, 1980; Granbakken *et al.*, 1991). Anhydrite scale of Well SC-1 became lengthened in formation section and thinned in thickness with enthalpy decreases as mentioned above. The extent of scale formation with log k in this model was consistent with the occurrence of the actual scale in Well SC-1.

Rate constants (log k) used in the simulations ranged from –6.00 to –4.00. In the mimimum value (–6.00 for log k) the maximum scale thickness was 0.4 mm, which means the scaling rate was quite slow. At the maximum value (–4.00) for log k) the maximum scale thickness was 36.1 mm. The calculation results of log k=-4.50 approximately agreed with the partial maximum reduction section of diameter in the 7-in. casing.

Flash points from PTS logging and WELBOR simulation corresponded with each other at about 1,200 to 1,300 m deep. The disappearance depth of scale from caliper logging was 1,530 m, which means that the results of scale simulations are remarkably different than the measured data.

Scaling had less affect on decreases of production rate at log k below –4.75. The rate of decrease in the production rate was only slightly less one year later at log k= -4.00. Consequently, it is concluded that scaling almost does not affect production rate below 20 mm of scale thickness.

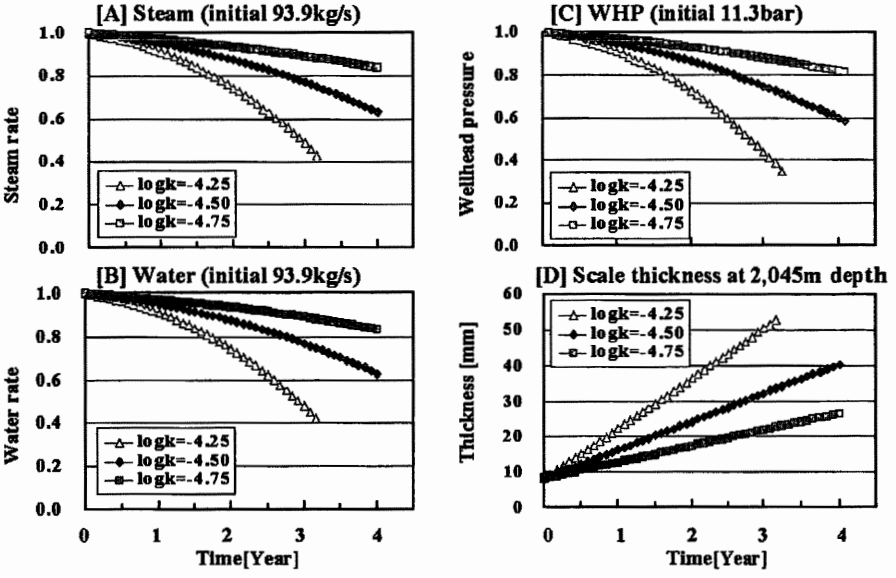

Figure 18. Results of simulations on the prediction during four years of steam [A] and water rates [B], wellhead pressure [C], and maximum thickness of scale [D]. [A], [B] and [C] are shown as the normalized values with the respective initial one.

Conclusions

In this paper the formation mechanism of anhydrite scale was analyzed and numerical simulations on the scaling and production performance were made, leading to the following findings:

1. A temperature inversion was observed near the bottom hole of well SC-1. Geothermal fluids feed from separate higher temperature (300°C) and a lower temperature (250 °C) zones. Anhydrite precipitates by mixing of the two different fluids.
2. Both the higher and lower temperature fluids that feed SC-1 are estimated to be saturated with respect to anhydrite. Mixing of the two fluids results in supersaturation of the anhydrite.
3. Fluid inclusions in anhydrite scale are composed of only liquid-rich inclusion, which indicates that the scale was formed from liquid in single phase prior to flashing. This information was consistent with the decrease of saturation index of anhydrite with flashing.
4. The concentration of Sr in anhydrite scale is much higher than predicted from experimentally determined equilibrium partitioning of Sr between aqueous and anhydrite phases. This indicates that the scale formed under non-equilibrium conditions, as seen in hot spring chimneys on the East Pacific Rise.
5. The flowing enthalpy of Well SC-1 has decreased with time. Occurrence of scale deposition has gradually changed a thick formation interval to one that is thinner, lengthened, and less in enthalpy.
6. In order to calculate scaling with time, it was assumed that the anhydrite precipitated as fluid deposits inside the casing pipe with uniform thickness. With the assumption, a mathematical model was developed using an isothermal non-steady plug-flow model. The analyses were made with scaling calculations coupled with wellbore simulations.
7. The simulation of history matching with variable rate constants led to the rate constant, log k=-4.50. Predictions using the optimum rate constants showed that the slight differences in the log k (±0.25) sensitively affected the magnitude of the decrease in steam rate. Changes in occurrence of scale deposition with enthalpy decreases, matched with the results of simulation with variable rate constants.

Acknowledgement

Authors thank Mitsubishi Materials Corporation and Hachimantai Geothermal Corporation for permission to publish this paper. They also wish to thank Dr. Haga of Tohoku University for many helpful comments and suggestions on modeling of scale formation.

References

Ajima, S. Todaka, N. and Muratake, H. (1998) An interpretation of smectite precipitation in production wells caused by the mixing of different geothermal fluids. Proceedings, Twenty-third Workshop on Geothermal Reservoir Engineering Stanford University, Stanford, California, January 26-28, 264-269.

Akaku, K. (1988) Geochemistry of mineral deposition from geothermal waters : Deposition processes of common minerals found in various geothermal fields and case study in the Fushime geothermal field. Chinetsu, 25, 44-61 (in Japanese with English abstract).

Armannsson, H. (1989) Predicting calcite deposition in Krafla boreholes. Geothermics, 18, 25-32.

Benoit, W. R. (1989) Carbonate scaling characteristics in Dixie Valley, Nevada geothermal wellbores. Geothermics, 18, 41-48.

Fournier, R.O. and Potter, R.W. (1982) A revised and expanded silica (quartz) geothermometer. Geothermal Resources Council Bulletin, 11, 3-12.

Granbakken, D., Haarberg, T., Rollheim, M., Ostvold, T., Read, P. and Schmidt, T. (1991) Scale formation in reservoir and production equipment during oil recovery. III. A kinetic model for the precipitation/ dissolution reactions. Acta Chemica Scandinavica, 45, 892-901.

Herras, E.B., Salonga, N.D. and Rossel, J.B. (2000) Mechanism of Calcite Carbonate Scaling in Mahanagdong Geothermal Field, Leyte, Philippines. GRC Trans., 24,?665-670.

Pritchett, J.W. (1985) WELBOR : A Computer Program for Calculating Flow in a Producing Geothermal Well. Rep. SSS-R-85-7283, S-Cubed.

Reed, M.H.(1982) Calculation of multicomponent chemical equilibria and reaction process in systems involving minerals, gasses and an aqueous phase. Geochimica Cosmochimica Acta, 46, 513-528.

Reed, M.J. (1989) Thermodynamic calculations of calcium carbonate scaling in geothermal wells, Dixie Valley geothermal field, U.S.A. Geothermics, 18, 269-277.

Rimstidt, J.D. and Barnes, H.L. (1980) The kinetics of silica-water reactions. Geochim. Cosmochim. Acta, 44, 1683-1699.

Shikazono, N. and Holland, H.D.(1983) The partitioning of strontium between anhydrite and aqueous solutions from 150°to 250°. Economic Geology, Monograph 5, 320-328.

Shikazono, N., Holland, H.D. and Quirk, R.F. (1983) Anhydrite in Kuroko Deposits : Mode of occurrence and depositional mechanisms. Economic Geology Monograph 5, 329-344.

Todaka, N., Kawano, Y., Ishii, H., and Iwai, N. (1995) Prediction of calcite scaling at the Oguni geothermal field, Japan : Chemical modeling approach. World Geothermal Congress 1995, 2475-2480.

Truesdell, A.H. and Lippmann, M.J. (1998) Effects of pressure drawdown and recovery on the Cerro Prieto Beta reservoir in the CP-III area., Proc. 23th Workshop on Geothermal Reservoir Engineering Stanford University, Stanford, California, January 26-28, 90-99.